

## Ferrous burden behaviour under nut coke mixed charge conditions

Gavel, Dharm Jeet; Adema, Allert; van der Stel, Jan; Sietsma, Jilt; Boom, Rob; Yang, Yongxiang

**DOI**

[10.1080/03019233.2020.1806678](https://doi.org/10.1080/03019233.2020.1806678)

**Publication date**

2020

**Document Version**

Final published version

**Published in**

Ironmaking and Steelmaking

**Citation (APA)**

Gavel, D. J., Adema, A., van der Stel, J., Sietsma, J., Boom, R., & Yang, Y. (2020). Ferrous burden behaviour under nut coke mixed charge conditions. *Ironmaking and Steelmaking*, 47(10), 1114-1126. <https://doi.org/10.1080/03019233.2020.1806678>

**Important note**

To cite this publication, please use the final published version (if applicable). Please check the document version above.

**Copyright**

Other than for strictly personal use, it is not permitted to download, forward or distribute the text or part of it, without the consent of the author(s) and/or copyright holder(s), unless the work is under an open content license such as Creative Commons.

**Takedown policy**

Please contact us and provide details if you believe this document breaches copyrights. We will remove access to the work immediately and investigate your claim.



## Ferrous burden behaviour under nut coke mixed charge conditions

Dharm Jeet Gavel , Allert Adema , Jan van der Stel , Jilt Sietsma , Rob Boom & Yongxiang Yang

To cite this article: Dharm Jeet Gavel , Allert Adema , Jan van der Stel , Jilt Sietsma , Rob Boom & Yongxiang Yang (2020) Ferrous burden behaviour under nut coke mixed charge conditions, Ironmaking & Steelmaking, 47:10, 1114-1126, DOI: [10.1080/03019233.2020.1806678](https://doi.org/10.1080/03019233.2020.1806678)

To link to this article: <https://doi.org/10.1080/03019233.2020.1806678>



© 2020 The Author(s). Published by Informa UK Limited, trading as Taylor & Francis Group



Published online: 22 Aug 2020.



Submit your article to this journal [↗](#)



Article views: 268



View related articles [↗](#)



View Crossmark data [↗](#)

## Ferrous burden behaviour under nut coke mixed charge conditions

Dharm Jeet Gavel <sup>a,b</sup>, Allert Adema<sup>c</sup>, Jan van der Stel<sup>c</sup>, Jilt Sietsma <sup>a</sup>, Rob Boom <sup>a</sup> and Yongxiang Yang <sup>a</sup>

<sup>a</sup>Department of Materials Science and Engineering, Delft University of Technology, Delft, Netherlands; <sup>b</sup>CRM Group, Liège, Belgium; <sup>c</sup>Research and Development, Tata Steel Europe, IJmuiden, Netherlands

### ABSTRACT

Effect of nut coke addition with ferrous burden (pellet and sinter mixture) is experimentally investigated under simulated blast furnace conditions. Nut coke mixing degree was varied (0, 20 and 40 wt-%) as a replacement of the regular coke. During smelting, the ferrous bed evolves through three distinct stages of shrinkage due to indirect reduction, softening and melting, respectively. Nut coke increases the reduction kinetics, limits softening and enhances iron carburization in the ferrous bed to affect all three stages. Additionally, nut coke physically hinders the sintering among the ferrous burden to keep the interstitial voids open, which exponentially increases the gas permeability. A significant impact of nut coke mixing occurs in the cohesive zone temperature range, which is decreased by 77°C upon addition of 40 wt-% nut coke. Various experimental results give supports for the extensive utilization of nut coke as a replacement of regular coke in the blast furnace.

### ARTICLE HISTORY

Received 22 June 2020  
Accepted 3 August 2020

### KEYWORDS

Ironmaking; blast furnace; nut coke; pellets; sinter; ferrous burden; softening-melting; permeability

### Introduction

The ironmaking blast furnace being a counter-current reactor, its efficiency is controlled by the gas permeability. Significantly high resistance to the gas flow is experienced during softening and melting (at cohesive zone) of ferrous raw materials in the blast furnace. The gas permeability in the cohesive zone can be increased by mixing nut coke (8–40 mm) with the ferrous raw materials [1,2]. On the one hand, this will provide an opportunity to utilize the undersize coke, which is generated due to the strict regular coke size (40–80 mm) demand from the blast furnace. On the other hand, nut coke utilization in the blast furnace is envisaged to increase the thermal reserve zone (TRZ) length [3], promote shaft efficiency [4,5] and enhance reduction kinetics [6,7].

Despite many advantages, nut coke is utilized in limited quantity (less than 30%) [4]. As the nut coke is utilized with the ferrous bed as a replacement of the regular coke, the regular coke layers get thinned. This may have a negative impact on gas permeability [2,8]. Thus, in our previous articles, a thorough investigation is presented on the effects of nut coke addition on the bed permeability [9]. Furthermore, the softening, melting and dripping behaviour from the

bed are discussed [10,11]. These studies are limited to the pellet bed only, considering iron ore pellets being the most common ferrous raw materials for iron production.

However, in the blast furnace, the ferrous raw material bed is generally a mixture of pellets and sinter. The mixing proportion of these raw materials is based on chemical and economic balance. These ferrous burdens are of different shape, size, chemistry and preparation history. When mixed charged, it could behave differently to completely transform the bed properties. Thus, a detailed investigation is presented on the physico-chemical behaviour of the individual (pellet and sinter) and mixed ferrous raw material in our previous article [12]. However, the effect of nut coke mixing is not discussed in that study.

Considering the principal aim of nut coke is to get utilized in place of regular coke to increase the bed permeability, it is crucial to understand the behaviour of nut coke mixed ferrous bed. In the present study, a thorough investigation is performed under simulated blast furnace conditions to understand the physicochemical characteristics of the ferrous burden (pellet and sinter) under nut coke mixed charge conditions.

### Materials and method

#### Raw materials

In the present study, commercially available iron ore pellets and sinter of size range 10–13 mm are utilized. Fluxed pellets of two types (types 1 and 2) and one type of iron ore sinter are mixed in 40:20:40 ratio to form a ferrous raw material bed (500 g). In the tests, the coke of size 10–15 mm and 20–25 mm are utilized as the nut coke and regular coke, respectively. The chemical analysis of the ferrous burden is given in Table 1.

The sample bed is organized inside the graphite crucible. In the sample without nut coke, the ferrous layer is sandwiched between the two regular coke layers (100 g). In the case of sample mixed with nut coke, the regular coke layer is proportionally removed. Consequently, the layer thickness of the regular coke decreases. In the experiments with nut coke, a maximum of 40 wt-% replacement of the regular coke is used in the mixture to avoid critical thinning of the regular coke layer.

#### Experimental conditions

Two sets of experiments were performed to understand the physicochemical behaviour of the ferrous bed

**Table 1.** Chemical analysis of the ferrous raw materials (XRF).

Sample	Fe(T)	CaO	SiO <sub>2</sub>	MgO	Al <sub>2</sub> O <sub>3</sub>	TiO <sub>2</sub>	MnO	P <sub>2</sub> O <sub>5</sub>	K <sub>2</sub> O
Pellet type 1	64.94	0.37	3.70	1.21	1.06	0.26	0.30	0.08	0.04
Pellet type 2	66.46	0.45	2.22	1.38	0.27	0.16	0.07	0.06	0.04
Sinter	57.42	11.50	4.31	1.24	1.19	0.16	0.43	0.10	0.03

**Table 2.** Thermal and gas profile followed during the experiments.

Step	Temperature range (°C)	Heating rate (°C min <sup>-1</sup> )	CO (%)	CO <sub>2</sub> (%)	H <sub>2</sub> (%)	N <sub>2</sub> (%)	Gas flow rate (NLPM*)
Step 1	20–400	7.0	0	0	0	100	5
Step 2	400–600	5.0	25	20.5	4.5	50	15
Step 3	600–950	5.0	30	15.5	4.5	50	15
Step 4	950–1050	1.2	33	12.0	5.0	50	15
Step 5	1050–1445	5.0	42	0	8.0	50	15
Step 6	1445–1505	5.0	42	0	8.0	50	15
Step 7	1505–1550	5.0	42	0	8.0	50	15
Step 8	1550–20	–5.0	0	0	0	100	5

\*NLPM – normal litre per minute.

with and without mixed nut coke. The experiments were conducted in the reduction softening and melting (RSM) apparatus under simulated blast furnace conditions. Detailed information about the experimental set-up is given in references [9,13–15].

### Smelting experiments

Smelting (20–1550°C) of the ferrous burden is carried out in RSM. The thermal and gas profile followed during the smelting experiments are given in Table 2. The smelting experiments are performed without and with nut coke replacement ratio of 20 and 40 wt-%. After smelting, the ferrous liquid dripped to get collected in the cup located in the RSM [10].

### Quenching experiments

The quenching for the sample bed was performed after a series of smelting experiments. In order to understand the prime reason for the ferrous bed

melting, samples are quenched (using nitrogen gas) close to the bed melting temperature ( $T_m$ ). For the ferrous bed without and with nut coke (40 wt-%), the bed is quenched at 1505°C (after step 6) and 1445°C (after step 5), respectively (Table 2). After cooling, the sample crucibles are cast using cold mounting resin and cut vertically into two halves for further analysis.

### Analysis

The cross-sections of the selected ferrous raw materials are visualized by using an optical microscope (Keyence VHX-5000). The chemical analyses of the pellets and sinter are measured with XRF (X-ray fluorescence, Panalytical, Axios Max), and the results are given in Table 1. The dripped samples collected in the cup after the smelting experiments are removed. After that, a portion of the sample is pulverized and magnetically separated (slag and

metal). The slag (non-magnetic portion) is analysed with XRF for the present elements and the metal (magnetic portion) is analysed for the carbon content with LECO (Carbon-Sulphur analyser, CS744). The elemental distribution present in the quenched sample is investigated using Energy Dispersive X-ray analysis (SEM-EDS, JSM-IT100). The thermodynamics software package 'Factsage 7.0' is utilized to calculate the equilibrium carbon concentration in iron at different temperatures.

## Results and discussion

### Typical ferrous bed characteristics

A typical trend of ferrous sample bed contraction and gas permeability under simulated blast furnace conditions is shown in Figures 1 and 2, respectively. Various stages of bed contraction and pressure drop are described in Tables 3 and 4, respectively.

### Bed shrinkage

Under the blast furnace conditions, the bed contraction of the ferrous raw materials evolves through three distinct stages (Figure 1) [9,16]. Generally, the three principal phenomena responsible for bringing these three stages are; indirect reduction, softening and melting [9].

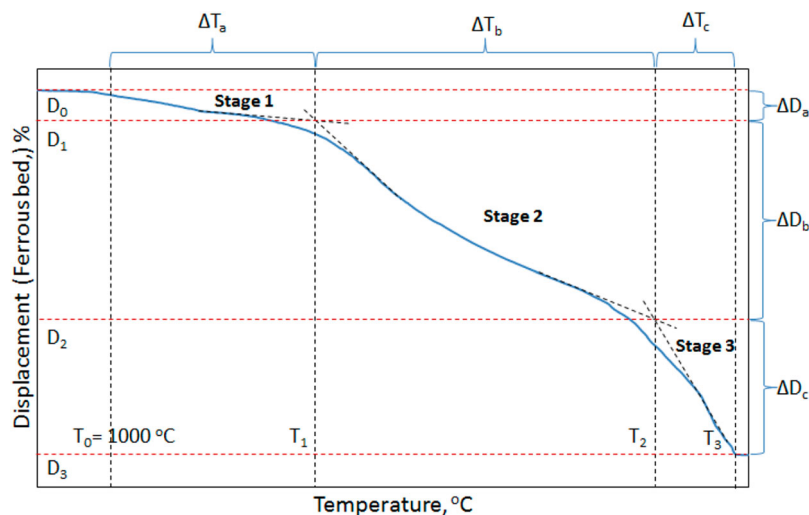


**Figure 1.** Stages of sample bed contraction under simulated blast furnace conditions.

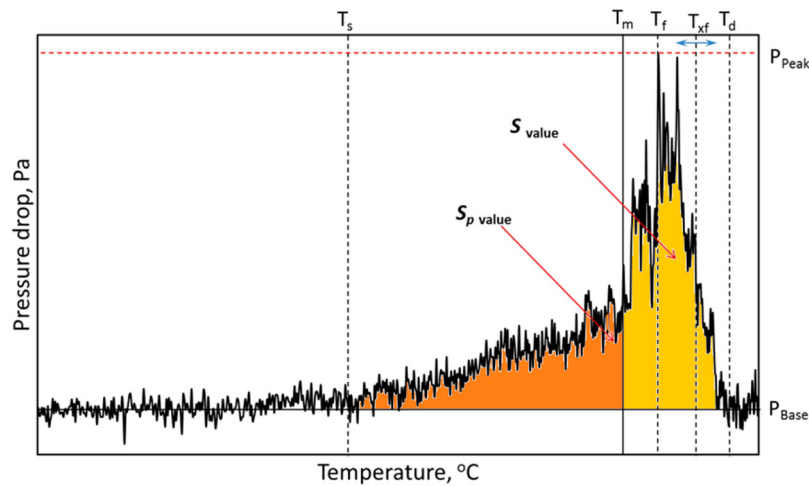


**Figure 2.** A typical pressure drop profile during the softening and melting of the ferrous burden.

### Gas permeability

A typical pressure drop profile during the softening and melting of ferrous raw materials under blast furnace conditions is shown in Figure 2 and various parameters are described in Table 4. A steady pressure difference across the sample bed means that a large density of pores is present in the bed, facilitating the passage for gas flow. As the reduction reaction proceeds, the iron nuclei form on the ferrous raw materials. Then with an increase in the temperature, these ferrous raw materials start to sinter individually (shell sintering) and among the other raw materials. Consequently, the interior of the ferrous raw materials becomes inaccessible for reducing gases [17].

Later, the unreduced iron oxide (FeO) starts to melt along with other flux (CaO and MgO) and gangue oxides (SiO<sub>2</sub>, Al<sub>2</sub>O<sub>3</sub>, etc.). Shortly after the start of melting, the gas starts to face resistance to flow across the bed. This is noticed by a gradual

increase in pressure drop from the  $P_{Base}$  value at the bed softening temperature ( $T_s$ ). The pressure drop continues to increase gradually as the sintering and local melting proceeds with an increase in the temperature.

Then, based on the carburization level achieved on the reduced ferrous sample surface, melting occurs to cause the shell breakout [14,15]. This is noted by a drastic increase in the pressure drop across the sample bed ( $T_m$ ). Then, the liquid fills up the open pores and voids to cause the flooding in the bed ( $T_f$ ). Thereafter, the liquid starts to move downward to drip out ( $T_{xf}$ ) of the sample bed. Consequently, the pressure drop value starts to recover back to reach the  $P_{Base}$  at bulk dripping temperature ( $T_d$ ) [18]. Thus, the total area under the pressure drop curve is a measure of overall resistance to the gas flow due to the softening and melting of the ferrous raw materials, which is denoted by 'S-value'. The area under the pressure drop curve till the start of bed

melting ( $T_m$ ) is a measure of total resistance to the gas flow during softening, which is denoted by 'S<sub>p</sub>-value'.

### Characteristics of ferrous burden (pellet and sinter mixture)

The characteristics of the individual pellets and sinter are discussed extensively in our previous articles [12]. In the present study, the ferrous burden is a mixture of iron ore pellets (40 % pellets type 1: 20 % pellets type 2) and sinter in 60:40 ratio. The chemistry of the ferrous burden is given in Table 1. The ferrous bed contraction and pressure drop profile is shown in Figure 3.

As discussed, three distinct stages of bed contraction are observed during the smelting of the ferrous burden. The first stage occurs predominantly due to the shrinkage of the individual pellets in the bed, which is a result of the indirect reduction reactions [9,16]. In the second stage, bed contraction starts with the rapid shrinkage, which

**Table 3.** Various parameters of sample bed contraction (based on Figure 1).

Symbol	Description	Unit
Stage 1	Individual ferrous raw material shrinkage due to reduction	-
Stage 2	Softening, sintering, and iron carburization	-
Stage 3	Melting of ferrous burden and melts dripping (molten iron and slag)	-
$T_0$	=1000°C. This temperature is defined as the end temperature of the thermal reserve zone in the blast furnace [1] and is taken as 1000°C.	°C
$T_1$	First stage end temperature. Identified by the intersection point of tangents drawn to stages 1 and 2 behaviour. $T_1$ represents the start of bed softening.	°C
$T_2$	Second stage end temperature. Identified by the intersection point of tangents drawn to stages 2 and 3 behaviour. $T_2$ represents the start of individual ferrous raw material melting in the bed.	°C
$T_3$	Third stage end temperature. Identified as the point after which no further bed contraction occurs.	°C
$\Delta T_a$	( $T_1 - T_0$ ), the temperature interval between the thermal reserve zone and the end of stage 1.	°C
$\Delta T_b$	( $T_2 - T_1$ ), the temperature interval of stage 2. Softening temperature range.	°C
$\Delta T_c$	( $T_3 - T_2$ ), the temperature interval of stage 3. Melting and dripping temperature range.	°C
$D_0$	Sample layer contraction at the start of an experiment (=0 %).	%
$D_1$	Bed contraction at the end of stage 1. Identified by the intersection point of tangents drawn to stages 1 and 2.	%
$D_2$	Bed contraction at the end of stage 2. Identified by the intersection point of the tangents drawn to stages 2 and 3.	%
$D_3$	Bed contraction at the end of stage 3. Identified as the point after which no further contraction occurs.	%
$\Delta D_a$	( $D_1 - D_0$ ), bed displacement in stage 1, occurs due to indirect reduction.	%
$\Delta D_b$	( $D_2 - D_1$ ), bed displacement in stage 2, occurs due to burden softening.	%
$\Delta D_c$	( $D_3 - D_2$ ), bed displacement in stage 3, occurs due to burden melting and draining.	%

**Table 4.** Process parameters of pressure drop in the sample bed.

Symbol	Description	Unit
$P_{Base}$	The base value of pressure drop before the softening-melting phenomenon.	Pa
$P_{Peak}$	The peak value of the pressure drop, the maximum pressure drop value observed during the test.	Pa
$T_s$	The softening point of the sample bed, the temperature at which the pressure drop value gradually increases above the $P_{Base}$ value.	°C
$T_m$	The melting point of the sample bed, the temperature at which the pressure drop across the bed starts to increase steeply.	°C
$T_f$	The flooding point, the temperature at which the pressure drop reaches the maximum.	°C
$T_{xf}$	The first liquid drop point, the temperature at which the first liquid drop is visualized (from the glass window) [10] dripping out of the sample bed.	°C
$T_d$	The dripping point, the temperature at which the pressure drop value reaches back to the base value as before the softening and melting.	°C
$S_p$	The area under the pressure drop curve, in the softening range just before the start of melting temperature ( $T_m$ ). It is a measure of resistance to the gas flow due to the burden softening [19].	Pa.°C
$S_{value}$	The complete area under the pressure drop curve, being a measure of the resistance offered by the sample to gas flow during softening and melting.	Pa.°C

occurs due to the start of pellet softening and sintering (within and among each other). Then, the sinter retards the rate of bed contraction to finally end the second stage at  $\sim 1505^\circ\text{C}$  ( $T_2$ ) with a bed displacement of 81 % ( $D_2$ ). The shift from the second stage to the third stage is gradual because the melting and dripping properties are controlled by the sinter [12].

The iron ore pellets contain a low amount of impurities and fluxes. Thus, the melting temperature of the pellet is controlled by the level of iron (pellet shell) carburization. However, the sinters are rich in gangue ( $\text{SiO}_2$  and  $\text{Al}_2\text{O}_3$ ) and fluxes ( $\text{CaO}$  and  $\text{MgO}$ ) contents (Table 1), which certainly affects its melting behaviour. Among these, the melting of the calcium-rich oxide ( $\text{CaO}$ ) is known to occur at very high temperatures [20]. Thus, when the melting of iron from pellets and sinter starts, the flow of liquid is retarded due to the presence of the solid slag forming mineral particles [12]. This indicates that when sinter and pellets are mixed charged, the bed contraction properties in the first and third stage is dominated by pellet and sinter, respectively. However, in the second stage, the bed shrinkage profile is governed by

pellets initially then it is controlled by the sinter softening behaviour.

The pressure drop profile across the bed starts to increase from  $P_{Base}$  (at  $1375^\circ\text{C}$ ), due to the softening and sintering of the ferrous burden. The pressure drop continues to increase gradually due to the presence of pellets. The slag in the pellet is mostly entrapped in the micropores present in the metallic shell and it is distributed in the core [17]. Consequently, at the time of bed softening, the interstitial voids around the pellets are open for the gas flow across the bed. However, once the pellet melting starts, the slag and metal fills-up the inter-particle voids to start the drastic increase in the pressure drop. In the ferrous bed, melting is observed to begin at  $1505^\circ\text{C}$ . Then, once the highest pressure drop is achieved ( $P_{Peak}$ ), it decreases due to the downward flow of liquid [18]. These suggest that similar to the pellet only bed [10], layer-wise carburization, melting and dripping occurs in the ferrous bed.

#### Effect of nut coke addition on ferrous burden contraction

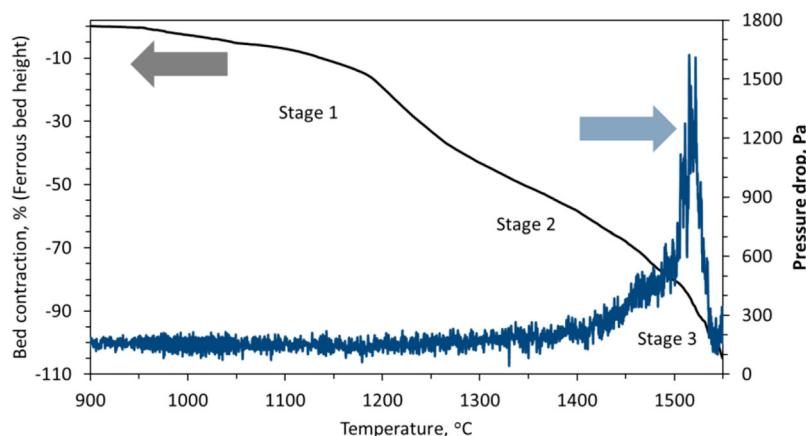
The influence of nut coke addition (20 and 40 wt-%) on the ferrous bed (60 % pellet and 40 % sinter mixture) shrinkage is

shown in Figure 4. The effect on the first stage of bed shrinkage is limited. A strong effect of the nut coke addition is observed in the second (softening) and third (melting and dripping) stage of bed contraction. A non-linear relationship is observed between the nut coke addition and the temperature ( $T_1$ ,  $T_2$  and  $T_3$ ) and displacement ( $D_1$ ,  $D_2$  and  $D_3$ ) characteristics. The effect of nut coke addition on different stages are discussed in the section below.

#### Effect of nut coke addition on stage 1 behaviour

In the first stage temperature range around  $1000^\circ\text{C}$ , iron ore pellet swelling might occur [16,21,22]. However, in the examined case of ferrous burden (pellet and sinter mixture) due to the load ( $9.8 \text{ N cm}^{-2}$ ) on the sample top and use of  $\text{H}_2$  gas for reduction, a limited swelling (less than 1 %) is observed (Figure 5). Owing to the close range, a clear effect of nut coke addition on the swelling is not established.

The end temperature of the first stage ( $T_1$ ), which represents the start of ferrous burden softening, increases from  $1157^\circ\text{C}$  to  $1163^\circ\text{C}$  with 40 wt-% nut coke addition (Figure 6). The nut coke enhances the reduction degree of

**Figure 3.** Characteristics bed contraction and pressure drop profile for the ferrous burden.

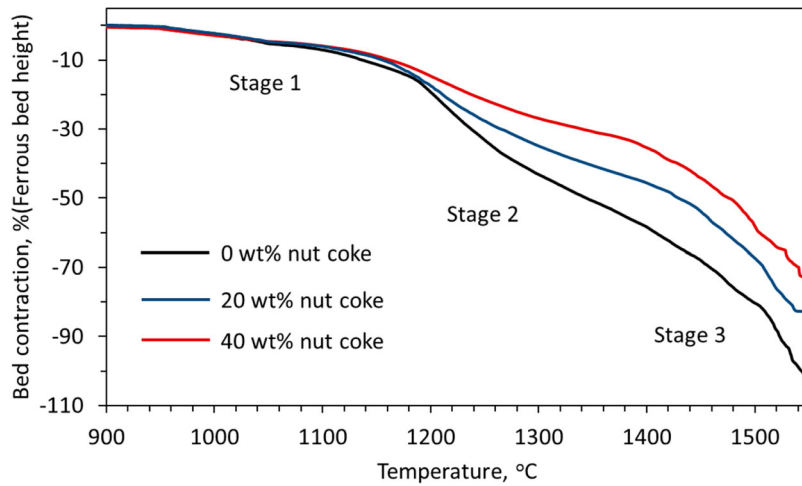


Figure 4. Effect of nut coke addition on the ferrous bed (pellet and sinter mixture) contraction.

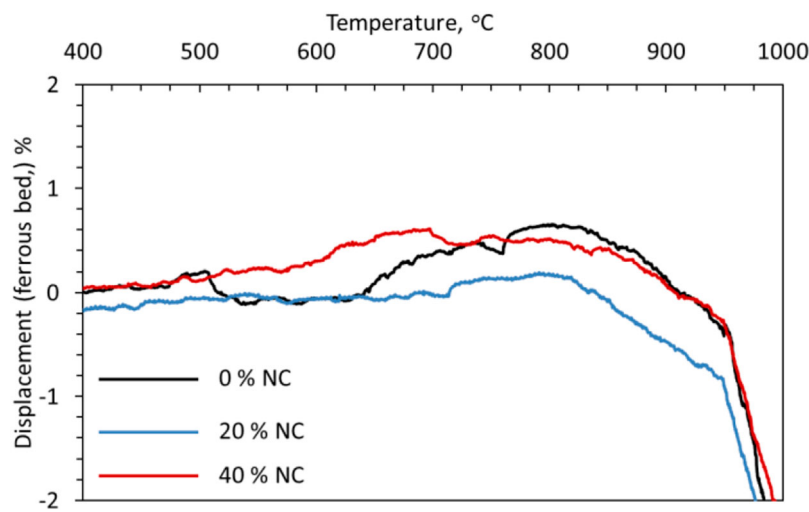


Figure 5. Effect of nut coke addition on the swelling behaviour of the ferrous bed (pellet and sinter mixture).

the ferrous burden to result in lower liquid (slag) formation, which increases the  $T_1$  temperature.

Despite the higher reduction degree achieved on the burden, the first stage bed contraction ( $D_1$ ) is observed to decrease from 12 % to 10 % with the increase in nut coke addition (Figure 6). The presence of nut coke in the

bed supports the structure and limits the sintering among the ferrous raw materials to undergo less contraction.

**Effect of nut coke addition on stage 2**

The nut coke mixing with the ferrous burden (pellet and sinter mixture) has a substantial effect on the second

stage of bed contraction (softening stage) (Figure 7). The second stage end temperature ( $T_2$ ), which represents the start of melting and the collapse of the individual ferrous burden, decreases by 98°C (1505°C to 1407°C) upon 40 wt-% nut coke addition (Figure 7). The  $T_2$  temperature is observed to decrease with an increase in added nut coke concentration.

The bed contraction in the second stage is observed to decrease from 81 % to 36 % upon 40 wt-% nut coke addition with the ferrous burden (Figure 7). One of the principal reasons for the bed shrinkage in the second stage is sintering among the ferrous burden [9,17]. The sintering results in slowing down of the reduction reaction by hindering the gas access to the unreduced portion of the ferrous burden (pellets and sinter). Consequently, the large volume of unreduced iron oxide (FeO) is left inside the ferrous burden. Now, as the temperature increases, the

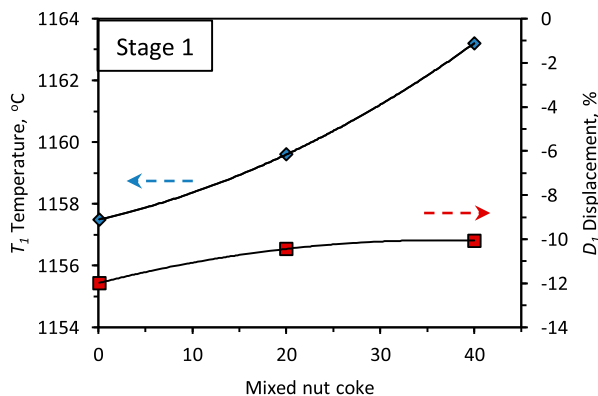
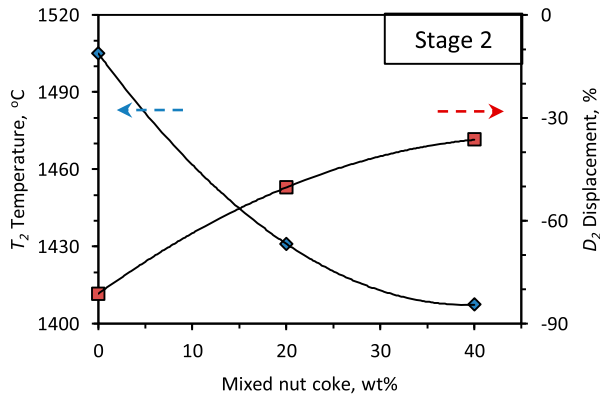


Figure 6. Effect of nut coke addition on the first stage of bed characteristics temperature ( $T_1$ ) and contraction ( $D_1$ ).



**Figure 7.** Effect of nut coke addition on the second stage bed characteristics temperature ( $T_2$ ) and contraction ( $D_2$ ).

melting of the FeO rich portion starts along with gangue ( $\text{SiO}_2$  and  $\text{Al}_2\text{O}_3$ ) to cause the 'reduction retardation' phenomena [6,23,24]. This melt lowers the strength of the ferrous burden, which cause the bed softening.

However, when nut coke is mixed with ferrous burden, it hinders the sintering among the ferrous burden, which allows the CO-rich gas to reach the interior of the burden to result in a higher reduction degree. Consequently, the 'reduction retardation' phenomena are minimized under nut coke mixed charge condition [6]. Now, as a result of formed metal on the ferrous raw materials, the bed strength increases to undergo comparative less contraction in the second stage [17].

In the nut coke mixed ferrous bed, due to the direct contact between coke and freshly reduced iron on the ferrous burden, the degree of the iron carburization is high. As a result, the melting temperature [25] of the reduced ferrous burden is observed to decrease with the nut coke addition (Figures 4 and 7). Therefore, the nut coke enhances the kinetics of metal

formation and carburization to lower the melting temperature of the ferrous bed. Consequently, the temperature and displacement range of the second stage is reduced with the increase in nut coke addition.

### Effect of nut coke addition on stage 3

The third stage ends with melting and draining out of the liquid from the bed, which is noticed from the maximum possible bed contraction achieved during the experiment (Figure 1). The end temperature for the third stage ( $T_3$ ) is observed to decrease from 1550°C to 1539°C with 40 wt-% nut coke addition (Figures 4 and 8). Owing to the early start and strong drainage rate in the presence of nut coke, the  $T_3$  temperature decreases with nut coke addition.

At the end of the third stage, liquid drains out to leave the unconsumed coke in the bed. Now due to the presence of unconsumed nut coke, the final bed displacement ( $D_3$ ) is observed to decrease with the nut coke addition (Figure 8).

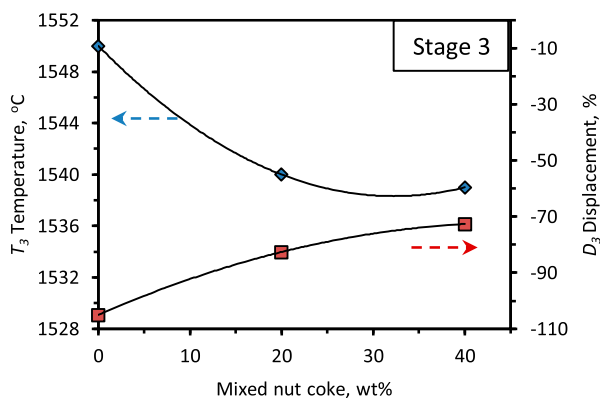


**Figure 8.** Effect of nut coke addition on the third stage bed characteristics temperature ( $T_3$ ) and contraction ( $D_3$ ).

### Bed displacement and temperature range

The first ( $\Delta T_a$ ) and third ( $\Delta T_c$ ) stage temperature range is observed to increase with the nut coke addition (Figure 9). However, the highest impact of nut coke addition is on the second stage (softening stage) (Figures 4 and 9). As discussed, the second stage temperature range is driven by the kinetics of iron oxide reduction and carburization of the reduced iron [9]. The presence of nut coke in the bed not only improves the reduction kinetics of the ferrous raw materials but also increases the carburization of the freshly reduced iron. Consequently, the melting of the ferrous burden shifts to the lower temperature [9,25], which results in a shortening of the second stage temperature range ( $\Delta T_b$ ).  $\Delta T_b$  is shortened by 103°C (347–244°C) upon 40 wt-% nut coke addition. Additionally, nut coke limits the sintering among the ferrous raw material particles by physically hindering the contact among them [17]. Moreover, nut coke acts as a frame at the time of burden softening to undergo less contraction. Consequently, in the second stage, the displacement range ( $\Delta D_b$ ) is decreased by 43 % (69 % to 26 %) upon 40 wt-% nut coke addition (Figure 9(b)).

Nut coke enhances the reduction degree of the ferrous burden to increase the first stage temperature range ( $\Delta T_a$ ).  $\Delta T_a$  is marginally increased by 6°C (157–163°C) with 40 wt-% nut coke addition in the ferrous bed (Figure 9 (a)). Despite a higher reduction in the ferrous burden due to the support provided by the nut coke in the bed, in the first stage, a decrease in the bed shrinkage range ( $\Delta D_a$ ) is observed. Similarly, the third stage displacement range ( $\Delta D_c$ ) is observed decreasing with nut coke addition.  $\Delta D_c$  is reduced by 12.5 % (36.2 % to 23.7 %) with 40 % nut coke addition in the ferrous bed (Figure 9(b)). The unconsumed nut coke present in the bed is the prime reason for the decrease in  $\Delta D_c$ .

### Effect of nut coke addition on ferrous bed gas permeability

The effect of nut coke addition on gas permeability (pressure drop) of ferrous bed (pellet and sinter mixture) is shown in Figure 10. In general, with the nut coke mixing in the ferrous bed,



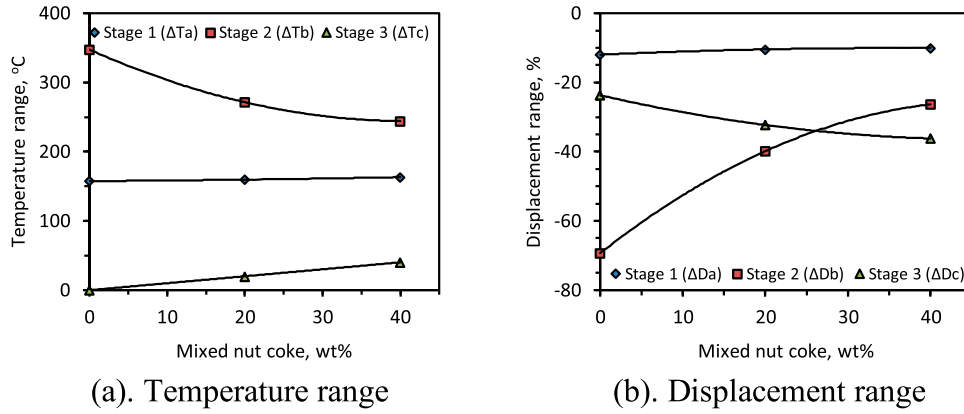


Figure 9. Effect of nut coke addition on temperature and displacement ranges of different stages. (a) Temperature range. (b) Displacement range

the high pressure drop regime is shifted to the low temperature range and the area under the curve is observed low. Various effects of the nut coke addition on the bed characteristic derived from pressure drop curves are discussed below.

**Effect on the bed characteristic temperatures**

The characteristic bed temperatures are examined from the measured pressure drop profiles according to the definition laid in Figure 2 and Table 4. The bed softening temperature ( $T_s$ ) is observed to increase by 44°C (1374–1418°C) upon 40 wt-% nut coke addition with the ferrous raw materials. The increase in softening temperature ( $T_s$ ) is due to the higher reduction degree achieved on the ferrous burden [17]. Additionally, the nut coke provides interstitial voids to accommodate the softening burden to delay the rise in a pressure drop across the bed.

The bed melting ( $T_m$ ) and dripping ( $T_d$ ) temperatures are noticed to decrease by 54°C (1505°C to 1451°C)

and 33°C (1539°C to 1506°C), respectively, upon 40 wt-% nut coke addition. In the presence of nut coke, the higher carburization achieved on the reduced ferrous burden is the principal reason for the decrease in the bed melting ( $T_m$ ) temperature [9]. The accessible pores and voids for gas flow due to the presence of nut coke in the bed facilities lower pressure drop ( $P_{Peak}$ ) and faster recovery to the  $P_{Base}$  value

(Figures 10 and 11). Consequently, dripping ( $T_d$ ) temperature decreases with nut coke addition.

**Effect on  $S_p$  and S-value**

During softening and melting of the ferrous raw materials, the pores in the bed start to get filled up by ferrous liquid to exert resistance against the gas flow. As a result, the pressure difference across the bed increases [26]. The

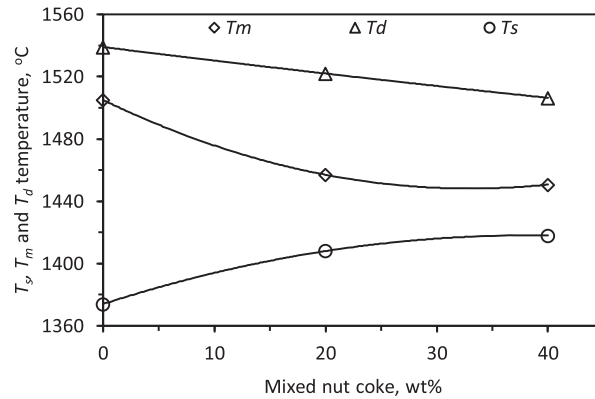


Figure 11. Effect of nut coke addition on the ferrous bed characteristic temperatures.

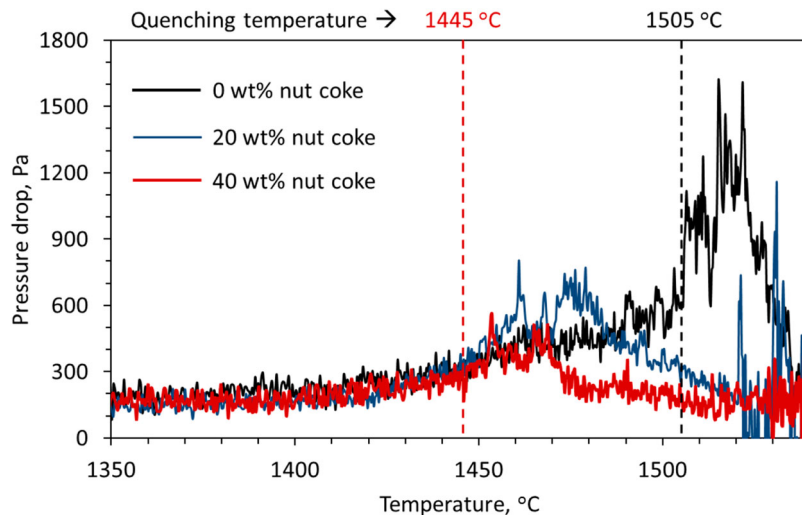
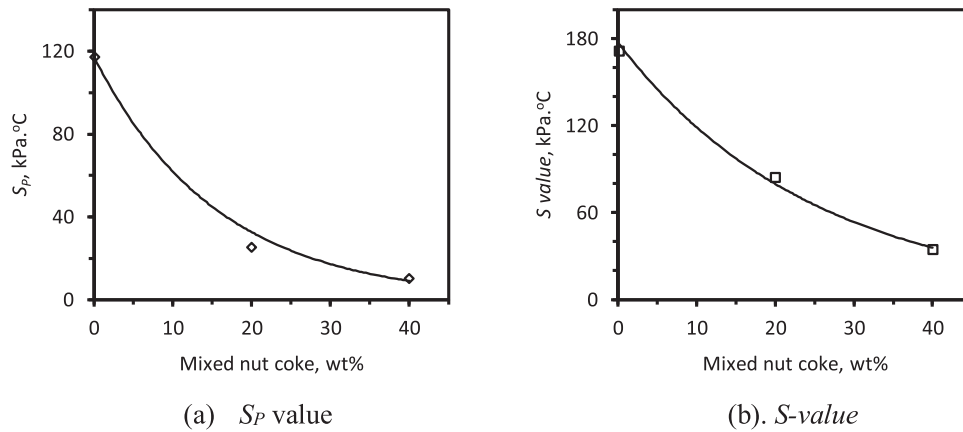
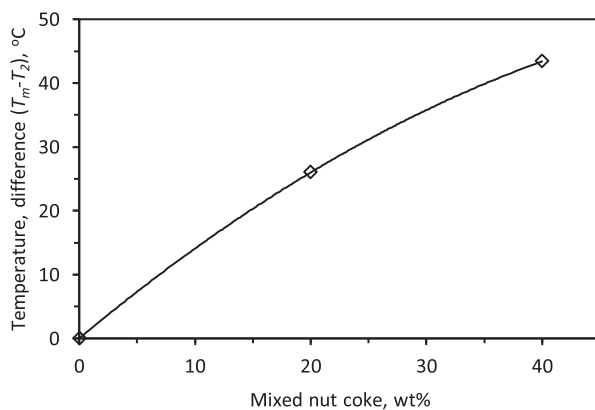


Figure 10. Effect of nut coke addition on the ferrous bed gas permeability (represented by the pressure drop across the sample bed). Identified bed quenching temperatures for the ferrous bed with (40 wt-%) and without nut coke at 1445°C and 1505°C, respectively.



**Figure 12.** Effect of nut coke addition on gas permeability (a)  $S_p$  value (a measure of resistance to gas flow during ferrous burden softening), (b)  $S$ -value (a measure of resistance to the gas flow during ferrous burden softening and melting).



**Figure 13.** Effect of nut addition on the temperature difference between individual burden melting ( $T_2$ ) and bed melting temperature ( $T_m$ ).

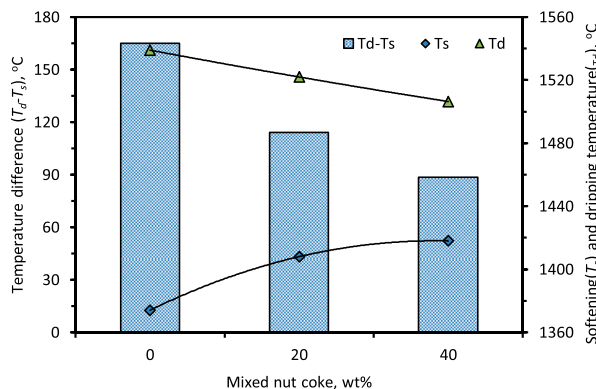


**Figure 14.** Effect of nut coke addition on cohesive zone temperature range ( $T_s$  to  $T_d$ ).

area under the pressure drop curve till the start of bed melting ( $T_m$ ) represents the resistance exerted to the gas flow due to the softening of the ferrous burden ( $S_p$ ). The complete area ( $S$ -value) under the pressure drop curve represents the total resistance exerted to gas flow during the softening and melting of the ferrous burden (Figure 2).

The  $S_p$  and  $S$ -value are observed to decrease with the nut coke addition (Figure 12). The nut coke present inside the bed remains solid at the cohesive

zone temperature conditions. These provide pores (on nut coke) and voids (interstitial) for the gas flow during bed softening and melting (Figure 12). Thus, the gas permeability improves (exponentially) with the nut coke addition in the ferrous raw materials bed.

#### Individual ferrous burden melting and bed melting

It is realized that for the ferrous bed mixed with nut coke, the melting ( $T_2$ )

temperature of the individual particles of ferrous raw material (pellet or sinter) is different from the melting ( $T_m$ ) temperature of the whole bed (bulk). It is found that the difference between the  $T_m$  and  $T_2$  temperature increases non-linearly by 43°C with 40 wt-% nut coke addition (Figure 13). At  $T_2$  temperature, the melting of individual ferrous material starts and by  $T_m$  temperature, the melt spreads substantially in the bed to cause a sharp increase in the pressure drop across the bed. As discussed before, the nut coke remains solid at the time of ferrous bed melting and accommodates the liquid in the interstitial voids to increase the bed melting temperature. However, in the absence of nut coke in the ferrous bed,  $T_2$  and  $T_m$  occur at the same temperature (Figure 13).

#### Effect of nut coke on softening and melting temperature range

The cohesive zone starts with the softening of the ferrous burden and ends with the melting and liquid dripping [1]. Thus during this process, limited pores are available in the bed for the gas flow. Consequently, reduced permeability occurs in the cohesive zone. In general, a narrow cohesive zone is desired for efficient blast furnace performance [26].

Considering the high-pressure drop regime spread between the  $T_s$  and  $T_d$  temperatures, it is expected that this temperature range will be close to the real cohesive zone in the blast furnace. The softening temperature increases and the dripping temperature decreases with the nut coke addition in the ferrous burden (Figure 14). Thus, the difference between the  $T_d$  and  $T_s$

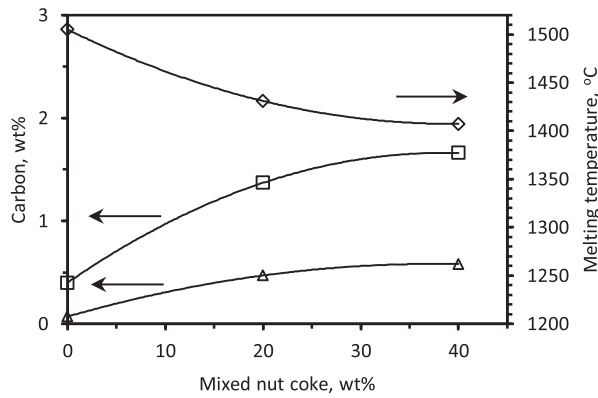


**Figure 15.** Effect of nut coke addition on liquidus and solidus carbon concentration (estimated).

temperature is reduced by 77°C (165°C to 88°C) upon 40 wt-% nut coke addition in the ferrous bed (Figure 14). Owing to the non-linear relationship of  $T_s$  and  $T_d$  temperatures with the nut coke addition, a similar relationship is also found between the cohesive zone temperature range and added nut coke content (Figure 14). Increased gas permeability and higher iron carburization are the principal reasons, which narrows the cohesive zone temperature range.

**Effect of nut coke addition on iron carburization**

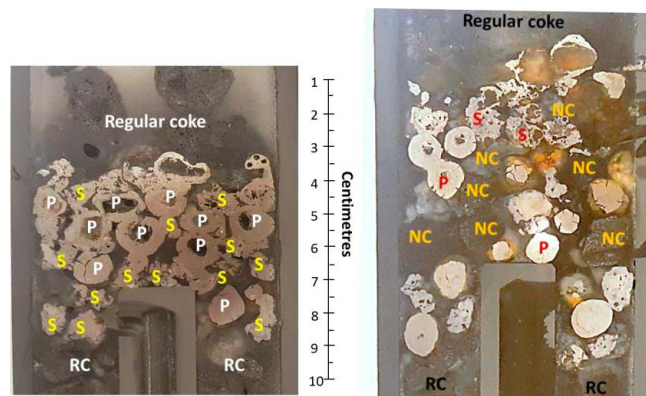
The melting temperature of the iron-carbon alloys decreases with the increase in the carbon concentration (for  $C < 4.3\%$ ) [25]. In the experiments under simulated blast furnace conditions, the freshly reduced iron gets carburized by CO gas [1] and mixed nut coke (present in close vicinity) [27]. Now, melting occurs in the bed, based on the carburization achieved on the freshly reduced iron. In the ferrous burden mixed with nut coke, iron

carburization is expected to be higher due to the increased gas permeability and presence of carbon (nut coke) inside the bed. Consequently, the melting temperature ( $T_2$ ) of the ferrous burden decreases with the increase in nut coke addition.

It is usually considered that various reactions that occur in the blast furnace are close to the equilibrium [1]. Thus, the liquidus and solidus carbon content at the start of melting can be estimated from the iron-carbon equilibrium diagram. Under the assumption that  $T_2$  is the ferrous burden melting point, the equilibrium liquidus and solidus carbon concentration are determined using Factsage 7.0 (Figure 15). When 40 wt-% nut coke is added, an increase in the liquidus carbon content by 1.26 wt-% (0.40 wt-%C to 1.66 wt-%C) is estimated. Similarly, the solidus carbon content is increased by 0.51 wt-%C (0.07 wt-%C to 0.58 wt-%C) upon 40 wt-% nut coke addition in the ferrous bed. At the start of ferrous burden melting, to have sufficient fluidity for the deformation and liquid flow, the carbon content is expected

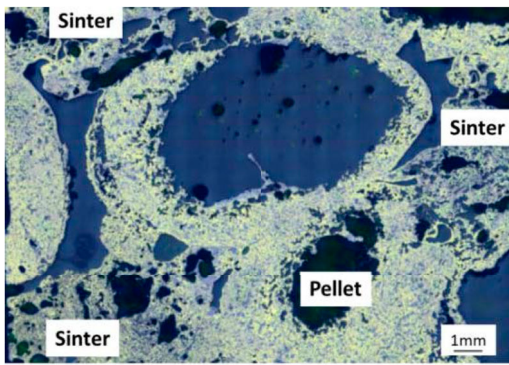
**Table 5.** Relationship summary on the effect of nut coke addition on the ferrous bed characteristics.

Parameters	Unit	Relationship	Equation $x =$ nut coke concentration (wt-%)	$R^2$
Stage 1 temperature ( $T_1$ )	°C	non-linear	$0.0019x^2 + 0.068x + 1157.5$	1.00
Stage 1 displacement ( $D_1$ )	%	non-linear	$-0.0015x^2 + 0.1071x - 11.991$	1.00
Stage 2 temperature ( $T_2$ )	°C	non-linear	$0.0635x^2 - 4.9949x + 1505.5$	1.00
Stage 2 displacement ( $D_2$ )	%	non-linear	$-0.0216x^2 + 1.9924x - 81.499$	1.00
Stage 3 temperature ( $T_3$ )	°C	non-linear	$0.0113x^2 - 0.725x + 1550$	1.00
Stage 3 displacement ( $D_3$ )	%	non-linear	$-0.0155x^2 + 1.43x - 105$	1.00
Bed melting temperature ( $T_m$ )	°C	non-linear	$0.0521x^2 - 3.4425x + 1505$	1.00
Flooding temperature ( $T_f$ )	°C	non-linear	$-0.03x^2 + 2.3x + 1374$	1.00
Dripping temperature ( $T_d$ )	°C	non-linear	$0.0017x^2 - 0.885x + 1539$	1.00
Dripping temperature ( $T_{dr}$ )	°C	non-linear	$0.0012x^2 - 0.7566x + 1528.1$	1.00
( $T_m - T_2$ )	°C	non-linear	$-0.0107x^2 + 1.515x - 1E-14$	1.00
( $T_d - T_s$ )	°C	non-linear	$12.7x^2 - 89.1x + 241.4$	1.00
Permeability resistance during softening ( $S_p$ )	Pa.°C	exponential	$117e^{-0.064x}$	0.97
Permeability resistance ( $S$ -value)	Pa.°C	exponential	$177.37e^{-0.04x}$	1.00

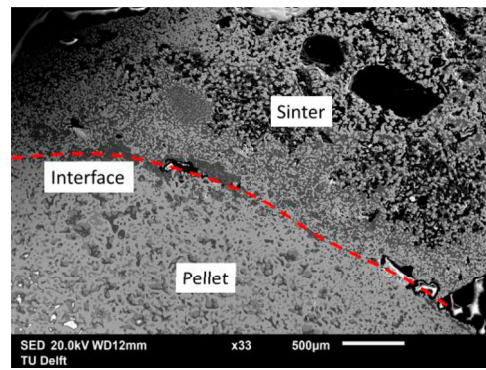


(a). Ferrous bed without nut coke, quenched at 1505 °C (b). Ferrous bed with 40 % nut coke, quenched at 1445 °C.

**Figure 16.** Photographs of the quenched ferrous bed with and without mixed nut coke (RC-regular coke, P-Pellet, S-Sinter and NC-Nut coke). (a) Ferrous bed without nut coke, quenched at 1505°C. (b). Ferrous bed with 40% nut coke, quenched at 1445°C.



(a). Optical micrograph from ferrous bed without nut coke



(b). Secondary electron micrograph at pellet and sinter interface.

**Figure 17.** Micrographs of the ferrous bed without nut coke. (a) Optical micrograph from ferrous bed without nut coke. (b) Secondary electron micrograph at pellet and sinter interface.

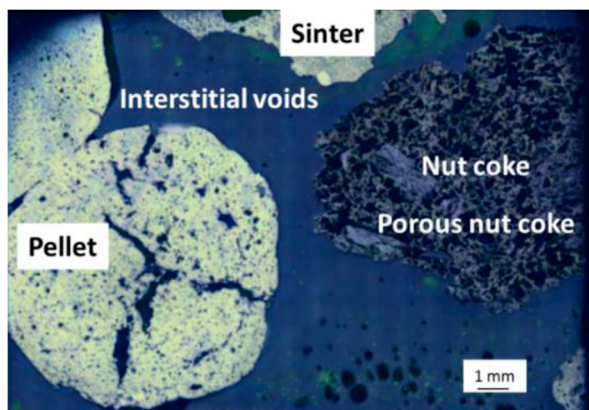


**Figure 18.** Optical micrograph from ferrous bed with mixed nut coke (Figure 16(b)).

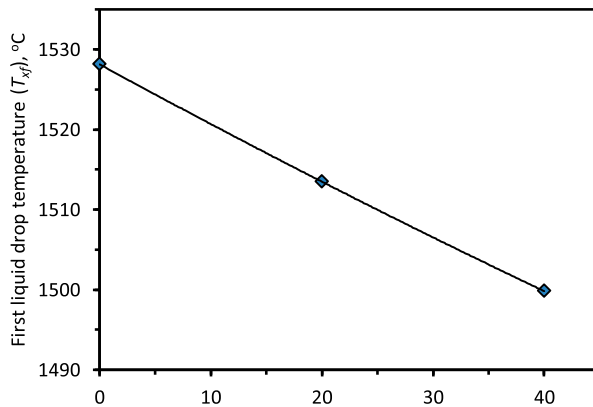


**Figure 19.** Effect of nut coke addition on the first liquid drop temperature ( $T_{xf}$ ).

to be close to the liquidus concentration instead of solidus concentration.

Based on the series of experiments under simulated blast furnace conditions, the effect of nut coke addition on various process parameters is studied in detail. As discussed earlier, a non-linear relationship is found for various key temperatures and displacement with the nut coke addition (Table 5).

This relationship is governed by the chemical function of coke (nut coke), which is to get utilized for the reduction of the ferrous burden (iron oxide) and iron carburization. For the given iron oxide content, with an increase in mixed nut coke, the demand for reducing and carburizing agent decreases. Additionally, the nut coke particle arrangement around the ferrous burden affects the physicochemical properties of the bed. Once the ferrous

raw material particle (pellet or sinter) is surrounded by one layer of nut coke, the second layer of nut coke around the ferrous particle can have a limited impact on the bed characteristics.

### **Morphology studies of the ferrous bed (pellet and sinter mixture)**

As discussed earlier, the permeability and cohesive zone properties improve with nut coke addition in the ferrous raw material bed. In order to understand and visualize the prime reason for such improvement, ferrous beds are quenched at the start of bed melting ( $T_m$ ). The ferrous bed without and with mixed (40 wt-%) nut coke are quenched at 1505°C and 1445°C, respectively, according to Figure 10. The photographs of the quenched ferrous bed is shown in Figure 16.

### **Ferrous bed in the absence of nut coke**

Photographs of the ferrous bed without nut coke quenched at 1505°C, is shown in Figure 16(a). A high degree of compaction is achieved on the ferrous bed. The iron ore sinter occupied the interstitial space around the pellets to close the inter-pellet voids. Additionally, close contacts among the sinter and pellets are observed (Figure 16(a)). The sintered structure of the ferrous raw material is evident under the optical microscope (Figure 17(a)). However, the interface between the sinter and pellet is apparent in the micrograph (Figure 17(b)). These indicate that the interaction between the sinter and pellet is limited to the interface region only. No bulk melting and intermixing between the

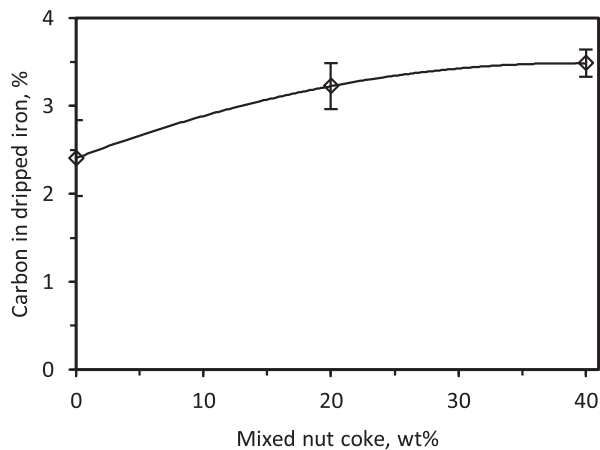


**Figure 20.** Effect of nut coke addition on carbon in the dripped metal.

sinter and pellet is observed till the bed melting temperature (1505°C).

In the pellet bed without nut coke, layer-wise melting is known to occur [10]. Similarly, in the quenched ferrous bed, the burden present in the top layer is observed to be significantly deformed (Figure 16). However, due to the heterogeneous shape of sinter particles, the deformation is not apparent. Additionally, the ferrous burden present in other layers is solid and able to hold their shape. Nevertheless, similar to the pellet-only burden, in the ferrous burden without nut coke, layer-wise carburization and melting are also expected to occur.

### Ferrous bed mixed with nut coke

The ferrous sample bed mixed with 40 wt-% nut coke is quenched close to the bed melting temperature of 1445°C (Figure 16). It is evident from the photograph that the nut coke acted as a frame to provide support to the ferrous bed. Consequently, a lower bed contraction is observed in the ferrous bed mixed with nut coke (Figures 4 and 16(b)). Additionally, the nut coke hindered the contact among the sinter and pellets to avoid the tight packing in the bed due to the sintering and softening of the ferrous burden (Figure 18). As a result, the pores and the voids are open to increase the gas permeability.

Consequently, reducing gases reach the unreduced regions in the ferrous

burden. Thus, the gas diffusion and chemical reaction are enhanced in the presence of nut coke in the bed [23]. Moreover, due to the direct contact of ferrous burden with nut coke, a higher degree of iron carburization occurs. Thus, the melting of the ferrous bed occurs simultaneously in the nut coke mixed ferrous bed.

Inside the bed, the presence of a thicker rim of the metallic shell on the pellets and sinter, clearly indicates that a higher degree of reduction is attained on the ferrous burden under nut coke mixed charge conditions (Figure 16). However, a few particles of sinter are found hollow on the top layer of the ferrous raw material bed. Sinter segregation could result in such behaviour.

### Dripped liquid

On the one hand, nut coke enhances the iron and carbon (coke) contact in the bed. On the other hand, the regular coke layer gets thinned, as the nut coke is added as the replacement of the regular coke. This might affect liquid interaction, hold-up and dripping characteristics [1]. Therefore, it is important to understand the effect of nut coke addition on the chemistry of the dripped liquid (metal and slag).

### Effect on first liquid drop temperature ( $T_{xf}$ )

The liquid drips out of the sample crucible and gets collected at the cups

located in the sample receiver [10]. The time and the temperature ( $T_{xf}$ ) of the first liquid drop are marked after visualizing the event from the glass window located at the receiver [10]. The ferrous liquid is observed to drip in the form of rivulets.

In the examined cases of ferrous burden, the temperature  $T_{xf}$  decreases with nut coke addition (Figure 19). As discussed, the nut coke enhances the degree of iron carburization to lower the melting point of the reduced iron [9,26]. The temperature  $T_{xf}$  is witnessed to decrease by 29°C (1528°C to 1499°C) upon 40 wt-% nut coke addition in ferrous bed. Additionally, the presence of a thinner regular coke layer in the case of nut coke mixed ferrous burden supports the earlier dripping of liquid from the bed. Once the liquid drop is formed in the bed, then while crossing the thinner regular coke layer, the probability of liquid hold up is also low. Consequently, the first liquid drop appearance temperature ( $T_{xf}$ ) decreases with nut coke addition in the ferrous bed.

### Effect of nut coke addition on liquid iron carburization

The carbon content in the dripped iron increased by 0.71 wt-% (from 2.78 to 3.49 wt-%) upon 40 wt-% nut coke addition in the ferrous bed (Figure 20). As discussed, the liquid iron is carburized during its flow over the coke bed [28]. In spite of the thinner regular coke layer present in the case of nut coke mixed ferrous burden, the carbon content in the dripped iron is observed to be higher than the iron produced in the absence of nut coke.

The presence of the sinter in the ferrous burden slows down the melting and dripping of liquid from the bed [12]. Thus, the reduced iron stays in bed for a longer time to interact with the coke. Thus, in the case of nut coke mixed ferrous burden, the presence of carbon (nut coke) in contact with the liquid iron enhances the iron carburization.

### Dripped slag chemistry

Dripped slag chemistry is shown in Table 6. No apparent effect of nut coke

**Table 6.** Dripped slag chemistry.

Nut coke	FeO, wt-%	CaO, wt-%	MgO, wt-%	SiO <sub>2</sub> , wt-%	Al <sub>2</sub> O <sub>3</sub> , wt-%	B <sub>2</sub> , C/S ratio	B <sub>3</sub> , (C+M)/S ratio	B <sub>4</sub> , (C+M)/(S+A) ratio
0	1.1	45.6	10.7	28.9	7.2	1.6	1.9	1.6
20	0.8	43.9	11.1	31.9	7.2	1.4	1.7	1.4
40	1.8	38.7	11.9	34.2	7.9	1.1	1.5	1.2

\*C – CaO, S – SiO<sub>2</sub>, M – MgO, A – Al<sub>2</sub>O<sub>3</sub>.

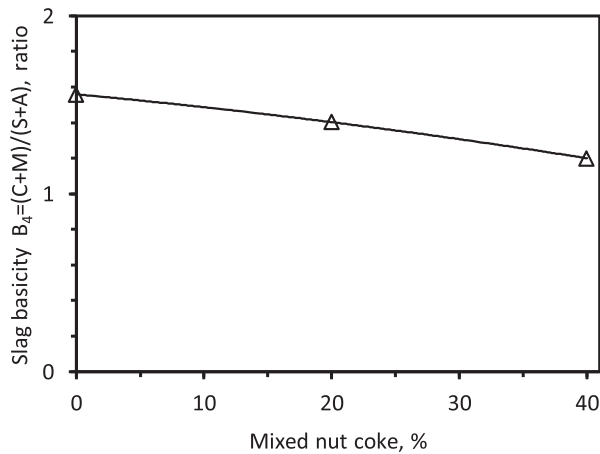


Figure 21. Effect of nut coke on dripped slag basicity.

Table 7. Non-dripped material (NDM) chemistry.

NC, wt-%	FeO, wt-%	CaO, wt-%	MgO, wt-%	SiO <sub>2</sub> , wt-%	Al <sub>2</sub> O <sub>3</sub> , wt-%	B <sub>2</sub> , C/S ratio	B <sub>3</sub> , (C+M)/S ratio	B <sub>4</sub> , (C+M)/(S+A) ratio
0	1.21	50.03	11.38	29.39	5.31	1.70	2.09	1.77
20	0.92	56.79	6.1	26.87	6.99	2.11	2.34	1.86
40	0.93	56.66	6.02	26.6	7.35	2.13	2.36	1.85

\*C – CaO, S – SiO<sub>2</sub>, M – MgO, A – Al<sub>2</sub>O<sub>3</sub>.

addition on the slag FeO content is observed. However, the FeO content in the dripped slag for all examined cases is noticeably very low (0.8–1.8 wt-%). As discussed, the presence of sinter retards the rate of melting and dripping to enhance the interaction between the coke and ferrous materials [12], which results in higher reduction.

A decrease in the dripped slag basicity ( $B_4$ ) is observed with the nut coke addition. This occurs due to the increase in silica and alumina content of the slag. As the nut coke is utilized during the experiment, which can increase the coke ash (SiO<sub>2</sub> and Al<sub>2</sub>O<sub>3</sub>) content in the slag to decrease the slag basicity (Figure 21). However, for certainty, this needs to be checked with total slag (dripped and non-dripped) and metal collected from the experiments.

The non-dripped material (NDM) is collected after the experiments from inside the crucible. Very high basicity is the reason for the non-dripping nature of this slag forming minerals (Table 7), which has a high liquidus temperature (above 1550°C) [20,28,29]. Consequently, these minerals are not able to melt and flow out of bed. The NDM from the ferrous bed without nut coke is observed to be high in silica. However, no apparent effect of nut coke addition is found on the non-dripped slag chemistry.

## Conclusions

The effect of nut coke addition on the ferrous burden (60% pellet: 40% sinter) is studied under simulated blast furnace conditions in the reduction, softening and melting (RSM) apparatus. After a series of smelting and quenching experimental investigations, the following conclusions can be drawn.

- (1) During smelting, the ferrous bed evolves through three distinct stages of bed shrinkage. Principal phenomena occurring in these stages are indirect reduction, softening and melting, respectively. Nut coke mixing with the ferrous burden affects all three stages of bed shrinkage. The impact of nut coke addition is significant in the second stage. Nut coke mixing enhances the reduction of ferrous burden and carburization of freshly reduced iron to shorten the second stage (by 98°C upon 40 wt-% nut coke).
- (2) In the ferrous bed without nut coke, though the sintering among the burden is limited to the interface region only at high temperature, it causes a significant loss of gas permeability. In the nut coke mixed bed, nut coke physically hinder the contact among the ferrous burden to limit the sintering. Consequently,

the gas permeability and softening temperature (44°C with 40 wt-% nut coke) increases upon nut coke addition.

- (3) At the time of softening and melting of ferrous burden, the nut coke acted as a frame to provide the pores and voids for the gas flow. Gas permeability (inverse of  $S_p$  and  $S$ -value) increases exponentially with nut coke addition in the ferrous bed.
- (4) Nut coke mixing with ferrous burden improves the physicochemical properties of the bed to decrease the cohesive zone temperature range ( $T_s$  to  $T_d$ ). It was reduced by 77°C upon 40 wt-% nut coke mixing with the ferrous burden.
- (5) A simultaneous and layer-wise melting occurs in the ferrous bed with and without mixed nut coke, respectively. The iron carburization occurs by direct contact with the coke. In the case of nut coke mixed ferrous burden, freshly reduced iron get carburized simultaneously to melt after that. However, when nut coke is absent, iron carburization and melting proceeds layer-wise.
- (6) A non-linear relationship is recognized between the added nut coke replacement ratio and various temperature and bed contraction characteristics.

These results give support for the extensive use of nut coke as a replacement of the regular coke in the iron making blast furnace.

## Acknowledgements

This research was carried out under project T41.5.13490 in the framework of the research programme of the Materials innovation institute (M2i) supported by the Dutch Government and metallurgical industry (Tata Steel). The project was conducted at the Department of Materials Science and Engineering (MSE) of the Delft University of Technology in the Netherlands.

## Disclosure statement

No potential conflict of interest was reported by the author(s).

## Funding

This work was supported by Materials Innovation Institute [grant number T41.5.13490].

## ORCID

Dharm Jeet Gavel  <http://orcid.org/0000-0003-0058-7190>

Jilt Sietsma  <http://orcid.org/0000-0001-8733-4713>

Rob Boom  <http://orcid.org/0000-0002-0519-0208>

Yongxiang Yang  <http://orcid.org/0000-0003-4584-6918>

## References

- [1] Biswas AK. Principles of blast furnace iron making – theory and practice. Brisbane: Cootha Publishing House; 1981.
- [2] Geerdes M, Chaigneau R, Kurunov I, et al. Modern blast furnace ironmaking: an introduction. Amsterdam: IOS Press; 2015.
- [3] Sato A, Aritsuka M, Yamagata Y, et al. The operation with larger amount of nut coke under high pulverised coal rate. *CAMP-ISIJ*. 1995;8(4):1064–1070.
- [4] Gavel DJ. A review on nut coke utilisation in the ironmaking blast furnaces. *Mater Sci Technol*. 2017;33(4):381–387. doi:10.1080/02670836.2016.1183073.
- [5] Babich A, Senk D, Gudenau HW. Effect of coke reactivity and nut coke on blast furnace operation. *Ironmaking Steelmaking*. 2009;36(3):222–229.
- [6] Mousa E, Senk D, Babich A. Reduction of pellets-nut coke mixture under simulating blast furnace conditions. *Steel Res Int*. 2010;81(9):706–715.
- [7] Mousa E, Babich A, Senk D. Effect of nut coke-sinter mixture on the blast furnace performance. *ISIJ Int*. 2011;51(3):350–358.
- [8] Ichikawa K, Kashihara Y, Oyama N, et al. Evaluating effect of coke layer thickness on permeability by pressure drop estimation model. *ISIJ Int*. 2017;57(2):254–261.
- [9] Gavel DJ, Adema A, van der Stel J, et al. Effect of nut coke addition on physico-chemical behaviour of pellet bed in iron-making blast furnace. *ISIJ Int*. 2019;59(5):778–786. doi:10.2355/isijinternational.ISIJINT-2018-580.
- [10] Gavel DJ, Adema A, van der Stel J, et al. Melting behaviour of iron ore pellet bed under nut coke mixed charge conditions. *ISIJ Int*. 2020;60(3):451–462. doi:10.2355/isijinternational.ISIJINT-2019-246.
- [11] Gavel DJ, Kwakernaak C, Sietsma J, et al. Carburisation and melting behaviour of iron ore pellet bed under nut coke mixed charge conditions. *Proceeding of Metec and 4th Estad*; 2019; Dusseldorf. P591.
- [12] Gavel DJ, Adema A, van der Stel J, et al. A comparative study of pellets, sinter and mixed ferrous burden behaviour under simulated blast furnace conditions. *Ironmak Steelmak*. June 2020. doi:10.1080/03019233.2020.1786644.
- [13] Song Q. Effect of nut coke on the performance of the ironmaking blast furnace [dissertation]. Delft: Delft University of Technology; 2013.
- [14] Gavel DJ, Adema A, van der Stel J, et al. Physicochemical behaviour of olivine iron ore pellets mixed with nut coke under simulated blast furnace conditions. *Proceeding of 8th International Congress on Science and Technology of Ironmaking – ICSTI*; 2018; Vienna. 523–529.
- [15] Song Q, Yang Y, Boom R. Effect of nut coke on the reduction behavior in iron-making blast furnace. *Baosteel Tech Res*. 2015;9:8–16.
- [16] Sternal J, Lahiri AK. Contraction and melt-down behaviour of olivine iron ore pellets under simulated blast furnace conditions. *Ironmak Steelmak*. 1999;26(5):339–348. doi:10.1179/030192399677194.
- [17] Gavel DJ, Song Q, Adema A, et al. Characterization of the burden behaviour of iron ore pellets mixed with nut coke under simulated blast furnace conditions. *Ironmak Steelmak*. 2020;47(2):195–202. doi:10.1080/03019233.2018.1510873.
- [18] Small J, Adema A, Andreev K, et al. Petrological study of ferrous burden-crucible interaction in softening & melting experiments: implications for the relevance of pressure drop measurements. *Metals (Basel)*. 2018;8(12):1082–1096. doi:10.3390/met8121082.
- [19] Bos M. Effect of nut coke in the cohesive zone properties of the ironmaking blast furnace [dissertation]. Delft: Delft University of Technology; 2009.
- [20] Allibert M, Gaye H, Geisler J, et al. Slag atlas. Dusseldorf: Verlag Staheisen; 1995.
- [21] Sharma T, Gupta RC, Prakash B. Swelling of iron ore pellets by statistical design of experiment. *ISIJ Int*. 1992;32(12):1268–1275.
- [22] Frazer FW, Westenberger H, Boss KH, et al. The relationship between basicity and swelling on reduction of iron-ore pellets. *Int J Miner Process*. 1975;2:353–365.
- [23] Bakker T. Softening in the blast furnace process: local melt formation as the trigger for softening of ironbearing burden materials [dissertation]. Delft: Delft University of Technology; 1999.
- [24] Kemppainen A, Ohno K, Iljana M, et al. Softening behaviors of acid and olivine fluxed iron ore pellets in the cohesive zone of a blast furnace. *ISIJ Int*. 2015;55(10):2039–2046. doi:10.2355/isijinternational.ISIJINT-2015-023.
- [25] Goldbeck OK. Iron-carbon, in: iron-binary phase diagrams. Berlin: Springer; 1982.
- [26] Nandy B, Chandra S, Bhattacharjee D, et al. Assessment of blast furnace behaviour through softening-melting test. *Ironmak Steelmak*. 2006;33(2):111–119. doi:10.1179/174328106X94744.
- [27] Nagata K, Kojima R, Murakami T, et al. Mechanisms of pig-iron making from magnetite ore pellets containing coal at low temperature. *ISIJ Int*. 2001;41(11):1316–1323.
- [28] Shatokha V, Velychko V. Study of softening and melting behaviour of iron ore sinter and pellets. *High Temp Mater Process*. 2012;31(3):215–220. doi:10.1515/htmp-2012-0027.
- [29] Hino M, Nagasaka T, Katsumata A, et al. Simulation of primary-slag melting behavior in the cohesive zone of a blast furnace, considering the effect of Al<sub>2</sub>O<sub>3</sub>, FeO, and basicity in the sinter ore. *Metall Mater Trans B*. 1999;30(4):671–683. doi:10.1007/s11663-999-0028-3.